Optimal Disturbances in Three-dimensional Boundary-Layer Flows

M. G. Byström[1], J. O. Pralits[2], A. Hanifi[1,3], P. Luchini[2] and D. S. Henningson[1]

[1]*Linné Flow Centre, KTH, Dept. of Mechanics, SE-100 44 Stockholm, Sweden*
[2]*Dipartimento di Ingegneria Meccanica, Università di Salerno, 84084 Fisciano (SA), Italy*
[3]*Swedish Defence Research Agency, FOI, SE-164 90 Stockholm, Sweden*

Abstract

In the present paper, two different approaches to compute the optimal disturbances in the quasi three-dimensional flows are presented. One of the approaches is based on the Multiple Scales method and the other one utilises the Parabolised Stability Equations.

1 Introduction

The classical approach used to predict the position of laminar turbulent transition in laminar boundary layers is based on the analysis of exponentially growing instabilities of infinitesimal amplitude. The position of transition is assumed to occur when the relative amplification of the perturbations first, at the most upstream position, reaches a certain value obtained from correlations with experimental studies in low freestream conditions. In experiments with moderate to high free-stream turbulence level, it has been noted that boundary-layer flows may undergo transition without the occurrence of any noticeable exponential instability (Tollmien-Schlichting waves). Instead, streaky structures have been observed in the form of streamwise elongated regions of defective velocity. Ellingsen & Palm [7] showed, with linear stability analysis of an inviscid channel flow, that three-dimensional perturbations without streamwise variation can lead to an instability that grows linearly rather than exponentially in time, and produces high- and low-velocity streaks. Landahl [15] showed that all inviscid shear flows can be unstable to three-dimensional perturbations and undergo temporal linear growth of the perturbation's kinetic energy. The physical mechanism of the formation of streaks is the lift-up effect, stemming from the fact that fluid elements tend to keep their horizontal momentum when displaced in the wall-normal direction, thus causing a streamwise-velocity perturbation. This basically inviscid algebraic growth was later shown to occur for a finite length of time in the presence of viscous damping, and thus denoted as transient growth. In the temporal framework several studies such as Butler & Farrell [3], Henningson et al. [13], Corbett & Bottaro [5, 6] have been performed for different parallel incompressible flows. Hanifi et al. [12] analysed, also in the temporal framework, the case of parallel compressible mean flow.

One of the few investigations of transient growth made so far concerning three-dimensional flows is the one performed by CB1 in which the mean flow was approximated by the Falkner-Skan-Cooke similarity solutions and the analysis was made using the temporal framework. They assumed a periodic behaviour of the streamwise and spanwise wavenumbers, and computed the optimal initial condition at time $t = 0$ such that a measure of the disturbance kinetic energy at a final time was maximised.

In two-dimensional flows the maximum amplification obtained from modal and non-modal analysis is given for quite different wavenumbers. As well known, the exponentially most amplified perturbations in incompressible boundary layers (regardless of the mean flow pressure gradient) are two dimensional. On the other hand, the maximum transient growth is found for a three-dimensional perturbation with the streamwise wavenumber equal to zero. In three-dimensional flows, the wavenumbers of the respective unstable regions might be very similar or even coincide. Corbett & Bottaro [6] (from here on denoted CB1) further showed that wavenumbers for which the unstable modal and non-modal results coincide correspond, in the modal analysis, to exponentially amplified perturbations almost aligned with the inviscid streamline. These perturbations are the so called crossflow vortices and exist both as steady and travelling waves.

In order for the theory of non-modal growth to be useful for transition prediction, since the perturbations on a wing in a real case are of convective type, the transient growth must be studied using a spatial framework. The maximum spatial transient growth (generated by the so called optimal perturbation) in two-dimensional incompressible flow was studied by Luchini [17, 18] and Andersson et al. [1] for the case of zero pressure gradient and by Tumin [20] including the pressure gradient. Tumin & Reshetko [21] also studied two-dimensional compressible flow in the presence of a pressure gradient. Transition prediction models have been proposed by Andersson et al. [1] which correlate the transition Reynolds number with the maximum spatial transient growth in the Blasius boundary layer.

The extension of the theory of spatial transient growth to incorporate also three-dimensional flows is still missing in the literature. A difficulty, which is immediately encountered, is how to model the perturbations. If a solution can be obtained using a single mode, i.e. if the contribution to the solution by all modes except the least stable one is zero or negligible, then this is a usually preferred since the computational cost is less or much less. However, how to model a certain perturbation is not a choice which can be made a priori but must be made considering the actual flow which one intends to analyse. In the analysis of two-dimensional incompressible mean flow, such as Luchini [17, 18] and Andersson et al. [1], it was clear due to the scale separation between the streamwise and the other two directions that a single-mode approach was not possible. In that case the linearized boundary layer equations were used and the parabolic system of equations were marched in the streamwise direction.

In this paper both the so called "single-mode" approach, and the extension to three-dimensional flows of the approach used by Luchini [18] and Andersson et al. [1] are presented. The first, which has been prepared by the authors Pralits and Luchini, is first derived and compared with the analysis made by CB1 for the temporal case in which a single-mode approach is exact, and the second has been prepared by Byström, Hanifi and Henningson.

2 Mean flow

In the present paper we study the growth of small disturbances in a developing boundary layer over a swept flat plate of infinite span where a pressure gradient is present in the chordwise direction. The scene of the survey is illustrated in figure 1, which also presents the utilized reference systems. The definitions are as follows: i) Cartesian coordinate system aligned with the plate, denoted by x, where x^1, x^2 and x^3 are the axes in the chordwise, the spanwise and the wall-normal directions, respectively. The corresponding velocity components are denoted U, V and W, respectively. ii) Cartesian coordinate system aligned with incoming flow, denoted by r. iii) Curvilinear, orthogonal coordinate system aligned with the external streamline, denoted by s. The axes s^1 and s^2 are, respectively, parallel and perpendicular to the streamline, and s^3 is normal to the plate. Hereafter, we will refer to these as the streamwise, cross-stream and wall-normal axes. The corresponding velocities will be denoted $U_{\rm s}$, $V_{\rm s}$ and $W_{\rm s}$, respectively. iiii) Non-orthogonal, curvilinear coordinate system which is utilized in the computations, as outlined in § 4.1. The coordinate axes ξ^1, ξ^2 and ξ^3 are, respectively, aligned with the streamline, parallel to the leading edge and normal to the plate. It can be noted that the wall-normal axis has the same direction in all four coordinate systems.

Our study will be restricted to flows with a fixed chordwise pressure gradient where the chordwise velocity at the boundary layer edge (superscript e) is given by a simple expression,

$$U^e = C\left(x^1\right)^m, \qquad (1)$$

where $m = \beta_{\rm H}/\left(2 - \beta_{\rm H}\right)$ and $\beta_{\rm H}$ is the Hartree parameter. Furthermore, it follows from the infinite span approximation that the spanwise component V^e is constant in the chordwise direction and that the flow is independent of the spanwise coordinate. For such simple 3D flows, often referred to as 2.5D, a family of similarity solutions exists for incompressible flows. They are called the Falkner–Skan–Cooke similarity solutions(see ref. [4]).

3 The single mode approach

In this section the approach to compute optimal disturbances in swept-wing flows by Pralits and Luchini is presented using the temporal framework. A similar analysis, as mentioned in the previous section, was made by CB1. A short description of their problem formulation is first made and then compared with the new "single-mode" approach used in the present analysis.

3.1 Temporal analysis

We consider a locally parallel laminar mean flow on a swept wing given by the Falkner-Skan-Cooke similarity solution, and the coordinate system s shown
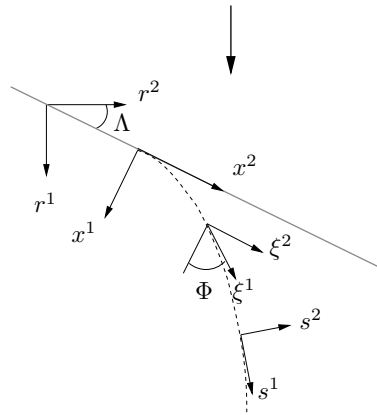
Figure 1: Flow over an infinite, flat plate with a sweep angle Λ.

in figure 1. Here, $Re = U_{S_0}\delta_0/\nu$ denotes the Reynolds number based on the streamwise velocity component, U_{S_0}, of the external flow at $s^1 = s_0^1$, and $\delta_0 = \sqrt{\nu s_0^1(m+1)/(2U_{S_0})}$. A flow decomposition $\tilde{u}(s^1, s^2, s^3, t) = U_S(s^3) + u'(s^1, s^2, s^3, t)$ is introduced into the Navier-Stokes equations for incompressible three-dimensional flow. Here, u' is an infinitesimal perturbation which is assumed to be periodic in the streamwise and spanwise directions. This can be written

$$u'(s^1, s^2, s^3, t) = u(s^3, t)\exp(i\alpha s^1 + i\beta s^2). \qquad (2)$$

The linearized Navier-Stokes equations, using the flow decomposition and the ansatz (2), can be written as

$$\mathbf{A}\frac{\partial \mathbf{q}}{\partial t} + \mathbf{B}\mathbf{q} = 0, \qquad (3)$$

where $\mathbf{q} = (\mathbf{u}, p)$, $\mathbf{u} = (u, v, w)$, and u, v, and w are the perturbation velocity components in the s^1, s^2, and s^3 directions respectively, and p is the perturbation pressure. The boundary conditions are chosen as non-slip on the wall and vanishing perturbation velocity in the freestream. If an exponential time dependence

$$\mathbf{u}(s^3, t) = \hat{\mathbf{u}}(s^3)\exp(-i\omega t) \qquad (4)$$

is introduced, equation (3) reduces to an eigenvalue problem with ω as the eigenvalue. We are interested in determining the initial condition $\mathbf{u}(s^3, 0) = \mathbf{u}_0(s^3)$ such that a *gain* given by

$$G(T) = \frac{E(T)}{E(0)} \qquad (5)$$

has its maximum value. Here $E(0)$, and $E(T)$, are the disturbance kinetic energies at time $t = 0$ and $t = T$. The disturbance kinetic energy is defined as $E(t) = \|\mathbf{u}\|^2$.

In CB1 optimal control theory was used to solve this problem by means of a gradient based optimization algorithm to find the optimal initial condition. The method is equivalent of using a steepest descent algorithm and the gradient was efficiently evaluated using the adjoint
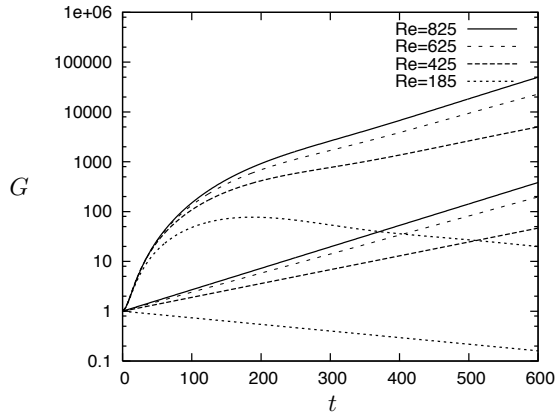
Figure 2: Gain $G(T)$ comparing optimal perturbations with exponentially growing perturbations varying the Reynolds number. Here, $\alpha = 0.0092$, $\beta = 0.461$, and $T = 600$, and the mean flow is given by $m = 0.46$, $\Lambda = 46.9$.
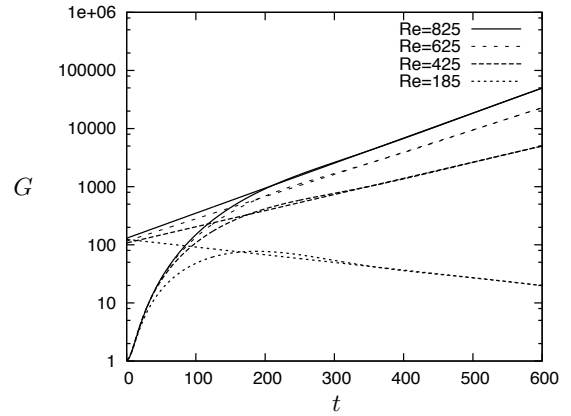
Figure 3: Gain $G(T)$ comparing optimal perturbations with the single-mode approach given by expression (9) varying the Reynolds number. Here, $\alpha = 0.0092$, $\beta = 0.461$, and $T = 600$, and the mean flow is given by $m = 0.46$, $\Lambda = 46.9$.

of equation (3).

In figure 2 a comparison between modal analysis assuming a time dependence according to expression (4) and optimal growth is made. The parameters for the three-dimensional mean flow are taken from CB1 and the wavenumbers α and β chosen such that the eigenvalue obtained from the Orr-Sommerfeld equation has a positive growth rate. The optimal perturbation was computed for a final time $T = 600$. It is interesting to note that the gain G of the optimal initial condition gives rise to a transient for $t < 200$ and for $t > 200$ has an evolution equal to that of the exponentially amplified perturbation. This has been verified by considering that for large times, in this particular case for t larger than 200, a relation between the evolution of the gain comparing the optimal initial condition and that of the exponentially amplified perturbation can be written $G_{opt} = KG_{exp}$, where K is a constant.

Further computations performed, varying the value of T while keeping all other parameters fixed, showed that K does not change as long as T is larger than approximately 200. It is important to note that the value 200 is depending on the parameters chosen. In a more general context we can instead consider that there exist a value for T above which the optimal initial condition for these types of flows will, after a short transient, evolve with an exponential behaviour. In fact, if one is interested in determining the gain due to the optimal initial condition for large values of T it is enough to capture the asymptotic evolution of G correctly. The task of computing the optimal perturbation for large values of T therefore consists in evaluating the gain using a modal analysis and, in addition, determine the value of K.

This can be obtained by considering that the initial condition that we aim to compute $\mathbf{u}_0(s^3)$ is the one giving the largest amplification. This can be written as a function of the left eigenvector of the Orr-Sommerfeld equation as

$$\mathbf{u}_0(s^3) = C\mathbf{v}_0(s^3), \qquad (6)$$

where $\mathbf{v}_0 = (u^\star, v^\star, w^\star)$, and $\mathbf{q}^\star_0 = (\mathbf{v}_0, p^\star)$ is the left eigenvector of the Orr-Sommerfeld equation. C is a con-

stant and function of the disturbance kinetic energy at $t = 0$, and $t = T$. The latter can be derived using optimal control theory, as in the work by CB1, in order to obtain the optimality condition. If we further consider that the perturbation considered takes the form of a single mode as

$$\mathbf{u}(s^3, t) = a_0\bar{\mathbf{u}}(s^3) \exp(-i\omega t), \qquad (7)$$

where a_0 denotes an initial, optimal, amplitude and bar denotes a chosen normalization, and the fact that also a_0 can be expressed as a function $\mathbf{v}_0$ as

$$a_0 = \mathbf{v}_0 \cdot \mathbf{u}_0. \qquad (8)$$

If the above mentioned normalization is chosen such that $\|\bar{\mathbf{u}}\|^2 = 1$ then the gain can be written

$$G(T) = \|\mathbf{v}_0\|^2 \exp(2\omega_i t), \qquad (9)$$

where ω_i is the imaginary part of the angular frequency. This expression is nothing but the gain computed for a single mode times a constant given by the value of $\|\mathbf{v}_0\|^2$. We denoted this factor the Algebraic amplification Factor (AF) and with the normalization used can take values $\|\mathbf{v}_0\|^2 \geq 1$. This means that when $\|\mathbf{v}_0\|^2 = 1$ the non-modal growth is zero. The corresponding optimal initial condition is given by expression (6), i.e. a function of the left eigenvector of the Orr-Sommerfeld equation.

In figure 3 the gain obtained from the single-mode approach using expression (9) is compared to the ones obtained from the optimal initial conditions shown in figure 2. It is clearly shown by these results that above a certain time the two different approaches coincide for various Reynolds numbers corresponding both to unstable and stable perturbations. It is interesting to note that the Algebraic amplification Factor is more or less the same for the different Reynolds numbers shown here. The values of AF can be read from figure 3 when $t = 0$.

In figure 4 the spanwise and wall-normal velocity components of the optimal perturbations are shown for two of the Reynolds numbers presented in figure 3. Note
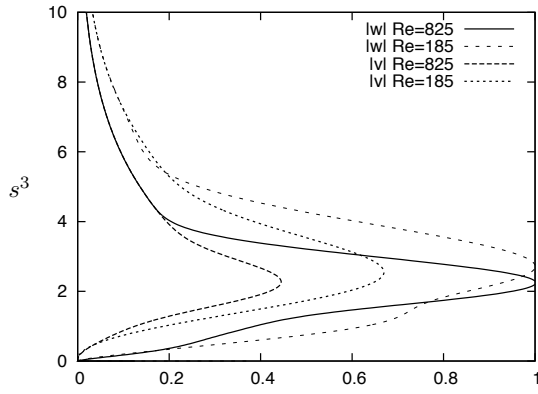
Figure 4: Spanwise (w) and wall-normal (v) velocity components of the optimal perturbation for $Re = 185$, and $Re = 825$. The profiles have been normalized such that $|w| = 1$. Here, $\alpha = 0.0092$, $\beta = 0.461$, and $T = 600$, and the mean flow is given by $m = 0.46$, $\Lambda = 46.9$.

that the same components of the left eigenvector for these two cases, which corresponds to the optimal initial condition of expression (9), are not shown as they coincide with the results of the optimal perturbations.

3.2 Spatial analysis

In this section the "single mode" approach presented in § 3.1 for the temporal framework is extended to the spatial framework in order to allow for the analysis of more realistic applications. In order to account for the growth of the boundary layer the linear stability analysis is here performed using the multiple scales analysis.

We assume a weak streamwise-dependency of the perturbation shape and express it as

$$\tilde{u}(X^1, x^2, x^3, t) = \hat{u}(X^1, x^3)\exp(i\beta x^2 - i\omega t). \quad (10)$$

where $X^1 = \epsilon x^1$ and ϵ is a small parameter. We now seek an asymptotic solution of the linearised equations when $\epsilon \to 0$ with the hypothesis that $\hat{u}(X^1, x^3)$ is the product of a exponential part and another which is expressed as a power series in ϵ as

$$\hat{u}(X^1, x^3) = \sum_n u_n(X^1, x^3)\epsilon^n \exp(i\phi(X^1)/\epsilon), \quad (11)$$

where $d\phi/dX^1 = \alpha$ is the complex wavenumber in the X^1 direction. If one substitutes equation (11) into the linearised equations and collects terms of equal powers in ϵ, one obtains a hierarchy of equations.

If one supposes that the scale of the rapid variation in the x^1 direction coincides with the length scale in the wall-normal direction (this is the hypothesis which has to be verified), then comparing the last one with the scale of the variation of the mean flow along the wall one obtains the parameter ϵ as a function of the Reynolds number, more precisely as $\epsilon = Re^{-1}$, where $Re = U_{ref}\delta/\nu$, and δ is proportional to the boundary layer thickness. These considerations deduce that ϵ is small and as a consequence one only has to consider the equations which corresponds to ϵ^0 and ϵ^1. The equations

are given as

$$O(\epsilon^0) \quad : \quad (\mathbf{A} + i\alpha\mathbf{I})\,\mathbf{q}_0 = 0, \quad (12)$$

$$O(\epsilon^1) \quad : \quad (\mathbf{A} + i\alpha\mathbf{I})\,\mathbf{q}_1 = -\frac{\partial\mathbf{q}_0}{\partial X^1} - \mathbf{C}\,\mathbf{q}_0. \quad (13)$$

The problem at order ϵ^0 is an eigenvalue problem. Equation (12) is actually the Orr-Sommerfeld equation, where $\mathbf{q} = (u, \hat{u}, v, \hat{v}, w, \hat{w}, p)$, and $\hat{u}, \hat{v}, \hat{w}$ are $i\alpha u, i\alpha v$ and $i\alpha w$, respectively. At order ϵ^1, the operator of the left hand side is identical to the one at order zero, while the matrix $\mathbf{C}$ contains the derivatives of the meanflow in the x^1 direction. According the theory regarding linear systems equation (13) does not have any solution if the right hand side does not satisfy an opportune condition, known as a compatibility condition. This condition consists in imposing that the right hand side is orthogonal to the left eigenvector $\mathbf{p}$ of the zero-order problem, that is

$$\mathbf{p}_0 \cdot (\frac{\partial\mathbf{q}_0}{\partial X^1} + \mathbf{C}\,\mathbf{q}_0) \quad = \quad 0. \quad (14)$$

The solution of equation (13) represents the correction to impose at order zero in order to account of the growth of the boundary layer in the direction of the flow. We now assume a decomposition of $\mathbf{q}_0$ as

$$\mathbf{q}_0(X^1, x^3) = a(X^1)\bar{\mathbf{q}}_0(X^1, x^3) \quad (15)$$

where $a(X^1)$ is the amplitude and $\bar{}$ denotes a chosen normalisation. If expression (15) is introduced into (14) we obtain an equation for the amplitude as

$$\frac{da}{dX^1}\mathbf{p}_0 \cdot \bar{\mathbf{q}}_0 + a(\mathbf{p}_0 \cdot \frac{\partial\bar{\mathbf{q}}_0}{\partial X^1} + \mathbf{p}_0 \cdot \mathbf{C}\bar{\mathbf{q}}_0) = 0, \quad (16)$$

which solution is written

$$a(X^1) = a_0 \exp\left(-\int_{X_0^1}^{X^1} \kappa(X^1)dX^1\right), \quad (17)$$

where a_0 is the amplitude at $X^1 = X_0^1$ and

$$\kappa = \frac{\mathbf{p}_0 \cdot \dfrac{\partial\bar{\mathbf{q}}_0}{\partial X^1} + \mathbf{p}_0 \cdot \mathbf{C}\bar{\mathbf{q}}_0}{\mathbf{p}_0 \cdot \bar{\mathbf{q}}_0}. \quad (18)$$

The final solution, using expression (15) and (17), can now be written

$$\tilde{\mathbf{q}} = a_0\,\bar{\mathbf{q}}_0 \times$$
$$\exp\left(\frac{i}{\epsilon}\int_{X_0^1}^{X^1} [\alpha(X^1) + i\epsilon\kappa(X^1)]dX^1 + i\beta x^2 - i\omega t\right), (19)$$

where $i\epsilon\kappa$ is the correction of the eigenvalue α due to the growth of the boundary layer. In the spatial framework, the optimal perturbation problem consists of finding the initial condition $\hat{\mathbf{u}}(X_0^1, x^3) = \hat{\mathbf{u}}_0(x^3)$ such that the gain

$$G(X_1) = \frac{E(X_1^1)}{E(X_0^1)} \quad (20)$$

has its maximum value. Here, X_0^1 and X_1^1 denote the initial and final positions of a certain interval of interest in the X^1 direction. This can be obtained by considering that the initial condition that we want to compute $\mathbf{u}_0(x^3)$ is the one giving the largest amplification. This

can be written as a function of the left eigenvector of the Orr-Sommerfeld equation as

$$\hat{\mathbf{u}}_0(x^3) = C\mathbf{v}_0(x^3), \qquad (21)$$

where $\mathbf{v}_0 = (u^\star, v^\star, w^\star)$, and $\mathbf{q}^\star_0 = (\mathbf{v}_0, p^\star)$ is the left eigenvector of the Orr-Sommerfeld equation. C is a constant and function of the disturbance kinetic energy at $X^1 = X_0^1$, and $X^1 = X_1^1$. The latter can be derived using optimal control theory, as in the work by CB1, in order to obtain the optimality condition. If we further consider that the perturbation considered takes the form of a single mode as expression (19) where a_0 denotes an initial, optimal, amplitude and $\bar{}$ denotes a chosen normalization, and the fact that also a_0 can be expressed as a function $\mathbf{v}_0$ as

$$a_0 = \mathbf{v}_0 \cdot \hat{\mathbf{u}}_0, \qquad (22)$$

then the gain, following the derivation used for the temporal framework with a normalization such that $\|\bar{\mathbf{u}}\|^2 = 1$, can be written

$$G(X_1^1) = \|\mathbf{v}_o\|^2 \exp\left(-\frac{2}{\epsilon} \int_{X_0^1}^{X_1^1} [\alpha_i(X^1) + \epsilon\kappa_r(X^1)]dX^1\right). \qquad (23)$$

Expression (23) is the optimal gain using a single mode approach in the spatial framework accounting for both modal and non-modal growth. The term $\|\mathbf{v}_o\|^2 \geq 1$ gives a measure of the non-modal growth where $\|\mathbf{v}_o\|^2 = 1$ means that the gain is governed only by exponential growth. A common approach to estimate the position of transition using a modal analysis is made by correlating the quantity $N = \ln(A/A_0)$ for the exponentially amplified perturbations with experiments performed in wind tunnels. Here, A is the perturbation amplitude at certain streamwise position, and A_0 denotes the amplitude at the first neutral position. In framework of the multiple scales theory, we can write

$$N = \frac{1}{\epsilon} \int_{X_0^1}^{X_1^1} [-\alpha_i(X^1)]dX + \int_{X_0^1}^{X_1^1} [-\kappa_r(X^1)]dX^1. \qquad (24)$$

Note here that the first term on the right hand side of expression (24) is the contribution from the local parallel analysis denoted N_l, and the second is the correction due to the slowly developing boundary layer here denoted N_{nl}. The same two terms can be derived from from expression (23) by taking the natural logarithm of the square root of $G(X_1)$. This is given as

$$\log[\sqrt{G(X_1^1)}] = \log(\|\mathbf{v}_0\|) + \frac{1}{\epsilon} \int_{X_0^1}^{X_1^1} [-\alpha_i(X^1)]dX^1$$
$$+ \int_{X_0^1}^{X_1^1} [-\kappa_r(X^1)]dX^1. \qquad (25)$$

In addition to the two terms given in expression (24) we have the natural logarithm of the square root of the Algebraic amplification Factor (AF) which in this case is given as $\log(\|\mathbf{v}_0\|) \geq 0$. It is important to note that this approach of computing the algebraic growth is new and has so far not been correlated with experimental data. The aim is to investigate if the new Algebraic amplification Factor can give additional information compared to the traditional N-factor in order estimate the postition of transition. An example using expression (25) is given
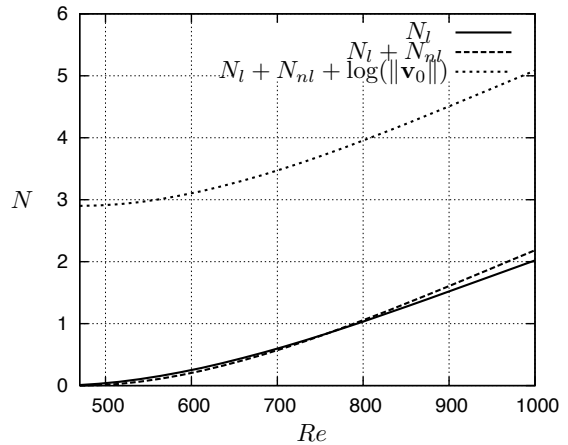
Figure 5: Relative amplification, expression (25), of stationary crossflow mode for a mean flow given by the parameters $\beta_H = 0.1$, $\Lambda = 45$ degrees, $\beta = 0.28$, $Re_0 = 825$.

in figure 5 for the case of a stationary crossflow mode and the mean flow given by the parameters $\beta_H = 0.1$, $\Lambda = 45$ degrees, $\beta = 0.28$ and $Re_0 = 825$. As expected the correction due to non-parallel effects is small. The algebraic amplification factor in this case, which is evaluated at the upstream neutral position, has a value of 2.9. However, preliminary results for the analysis of stationary modes show that the algebraic amplification factor depends both on the waveangle and the mean flow.

4 PSE approach

In this section, the approach based on the Parabolised Stability Equations (PSE) used by Byström, Hanifi & Henningson is presented.

4.1 Formulation

First, we discuss the appropriate scaling, coordinate system and disturbance equations for our studies of transient growth in the Falkner–Skan–Cooke boundary layer. Herein, R denotes the Reynolds number $R = U_0\delta_0/\nu$ where U_0 is the chordwise velocity of the external flow at $x^1 = x_0^1$ and $\delta_0 = \sqrt{\nu x_0^1/U_0}$. Andersson et al. [1] and Luchini [18] employed the linearized disturbed boundary layer equations (LDBLE) in their independent studies of transient growth in the Blasius boundary layer. This analysis was later extended to the Falkner–Skan boundary layer by Levin & Henningson [16], who presented a comparative study of algebraically growing streaks, governed by the LDBLE, and exponentially growing TS-waves governed by the PSE. Both set of equations are derived from the linearized Navier–Stokes equations, with the disturbance $\tilde{q}$ assumed to be of the form

$$\tilde{q}\left(x^1, x^2, x^3, t\right) = \hat{q}\left(x^1, x^3\right) \exp\left(i\theta\right) \qquad (26)$$
$$\theta = \int \alpha\, dx^1 + \beta x^2 - \omega t. \qquad (27)$$

where $\hat{q}$ is a complex amplitude function, α and β are the chordwise and spanwise wavenumbers, respectively, and ω is the angular frequency. The principal difference

is that the PSE accounts for disturbances with a rapid, oscillatory variation in the chordwise direction while the LDBLE assumes a slow, non-oscillatory variation, hence the chordwise wavenumber is zero. Due to the different choices of scaling, the LDBLE is a Reynolds-number independent set of equations, identical to the Görtler equations with zero Görtler number (see refs. [8] and [10]), while the PSE are Reynolds-number dependent.

The PSE has successfully been employed in studies of stationary cross-flow modes, see e.g. the comparison with DNS results in [14]. According to [6], the physical mechanism behind transient growth in the Falkner–Skan–Cooke boundary layer is similar to that of the exponentially amplified cross-flow modes. Bagheri & Hanifi (2007) (paper + private communication) modified the PSE to obtain a parabolic set of equations, which was employed to calculate the algebraic growth of longitudinal vortices. They considered disturbances with infinite chordwise wavelength and kept $\mathcal{O}\left(R^{-2}\right)$ terms, namely $W_{x^1}\hat{u}$ (W and $\hat{u}$ are the wall-normal and chordwise components of the meanflow and the disturbance, respectively) in the wall-normal momentum equation. Calculations showed that this term has a significant impact on algebraic instabilities but no bearing on the exponentially growing TS-waves. Furthermore, Bagheri & Hanifi [2] omitted the chordwise gradient of the disturbance pressure, $\hat{p}_{x^1}$, from the chordwise momentum equation. This term, associated with rapid oscillations in time, is neglectable for the stationary disturbances associated with the maximum algebraic growth. The calculated energy growth agreed very well with that reported by Levin & Henningson [16].

Herein we will employ a similar set of parabolic equations to study transient growth in the Falkner–Skan–Cooke boundary layer. In order to do so, we must however first find an integration path along which the wavenumber can be set to zero. It is well known that disturbances tend to be aligned with the external streamline in 3D boundary layers, i.e. the streamwise wavenumber is zero. We will therefore formulate the disturbance equations for the non-orthogonal coordinate system ξ where the first axis ξ^1 is aligned with the external streamline.

Under the infinite span approximation the mean flow is considered to be independent of the spanwise coordinate ξ^2. By subtracting the equations for the mean flow and removing the products of disturbances, a linearized set of disturbance equations is obtained. The disturbances are assumed to be spanwise periodic and non-oscillatory in the streamwise direction, hence the streamwise wavenumber is set to zero. Herein we will only consider stationary disturbances, the total disturbance (26) can thus be simplified to

$$\tilde{q}\left(\xi^1,\xi^2,\xi^3\right) \;=\; \hat{q}(\xi^1,\xi^3)\exp\left(i\beta\xi^2\right). \qquad (28)$$

Furthermore it is assumed that the variation along the streamline is weak, i.e. $\partial/\partial\xi^1 \sim \mathcal{O}\left(R^{-1}\right)$. Note that here we modify the PSE by assuming that W is of the same order as the other velocity components of the meanflow. Introducing the disturbance (28) into the linearized equations and dropping terms associated with the streamwise pressure gradient yields a parabolic set of disturbance equations:

$$\boldsymbol{A}\hat{\boldsymbol{\phi}} + \boldsymbol{B}\frac{\partial\hat{\boldsymbol{\phi}}}{\partial\xi^3} + \boldsymbol{C}\frac{\partial^2\hat{\boldsymbol{\phi}}}{\partial\xi^3\partial\xi^3} + \boldsymbol{D}\frac{\partial\hat{\boldsymbol{\phi}}}{\partial\xi^1} \;=\; \boldsymbol{0}, \qquad (29)$$

where $\hat{\boldsymbol{\phi}}$ is a vector containing disturbance quantities. The elements of the matrices $\boldsymbol{A}$, $\boldsymbol{B}$, $\boldsymbol{C}$, $\boldsymbol{D}$ can be found in Byström [9]. The velocity disturbances are subjected to no-slip boundary conditions and vanishing in the freestream. Furthermore, the initial conditions must be specified at the inlet. Together with the boundary and initial conditions, the disturbance equations (29) forms an initial-boundary-value problem that can be solved through a downstream marching procedure. A detailed description of the numerical scheme employed herein can be found in Hanifi et al. [11].

4.2 Adjoint optimization procedure

We are interested in identifying the initial disturbance that is optimal in the sense that it maximizes the growth of the disturbance energy as defined in equation (20). Following the works of Andersson et al. [1] and Luchini [18], we will employ an adjoint-based optimization procedure to identify the initial disturbance ϕ_{in} which maximizes the energy growth (20).

The initial-boundary value problem (29) is linear and homogeneous, and can be regarded as an input-output problem, where the disturbance equations (29) acts as a linear operator $\mathcal{A}$ on the initial disturbance ϕ_{in} (the input) to produce a downstream disturbance ϕ_{out} (the output) at the outlet

$$\phi_{\text{out}} = \mathcal{A}\phi_{\text{in}} \qquad (30)$$

Employing operator theory, it can be shown that the maximum growth G_{max} is the largest eigenvalue λ_{max} of the eigenvalue problem

$$\mathcal{A}^*\mathcal{A}\phi = \lambda\phi \qquad (31)$$

and the optimal initial disturbance ϕ_{in} is the corresponding eigenvector ϕ. Here $\mathcal{A}^*$ represents the adjoint to the operator $\mathcal{A}$. To solve the eigenvalue problem (31) and determine the optimal disturbance, we employ power iterations of the form

$$\phi^{n+1} = \mathcal{A}^*\mathcal{A}\phi^n \qquad (32)$$

The action of the operator $\mathcal{A}$ on an initial disturbance ϕ^n, i.e. $\mathcal{A}\phi^n$, is given by the disturbance equations (29). Here, the operator $\mathcal{A}^*$ is the adjoint of the operator $\mathcal{A}$ and can be written as

$$\tilde{\boldsymbol{A}}\boldsymbol{\phi}^* + \tilde{\boldsymbol{B}}\frac{\partial\boldsymbol{\phi}^*}{\partial\xi^3} + \tilde{\boldsymbol{C}}\frac{\partial^2\boldsymbol{\phi}^*}{\partial\xi^3\partial\xi^3} - \tilde{\boldsymbol{D}}\frac{\partial\boldsymbol{\phi}^*}{\partial\xi^1} = \boldsymbol{0}, \quad (33)$$

where $\boldsymbol{\phi}^*$ are the adjoint variables. The bondary and initial conditions as well as the enteries of matrices $\tilde{\boldsymbol{A}}$, $\tilde{\boldsymbol{B}}$, $\tilde{\boldsymbol{C}}$ and $\tilde{\boldsymbol{D}}$, are given in ref. [9] . The adjoint equations must be marched in the upstream direction. The initial conditions must therefore be set at the outlet $\xi^1 = \xi^1_{\text{out}}$.

As outlined in § 4.1, the calculations are carried out under the assumption that the wavenumber is zero along the ξ^1 -axis. This axis is aligned with the external streamline, since it is known that disturbances in 3D boundary layers evolves nearly along this line. Calculations with the present implementation does however reveal that the disturbances are not perfectly aligned with the streamline. This small deviation is equivalent to a small, but non-zero wavenumber with respect to the ξ^1-axis. Although such a small deviation will only cause neglectable errors locally, the cumulative effect may be significant when the disturbance equations (29) are in-

tegrated over a long streamwise distance. Therefore, an iterative procedure was utilized to identify the streakline (the disturbance trajectory as the nline which follows the maximum of the streamwise disturbance velocity).

4.3   Results

In this section we will study the optimal disturbances in boundary layers within the Falkner–Skan–Cooke family with a sweepangle of $\Lambda = 45°$. We consider both an accelerated flow with a chordwise pressure gradient of $\beta_{\mathrm{H}} = 0.1$ and a retarded flow; $\beta_{\mathrm{H}} = -0.05$. The chordwise velocity at the boundary layer edge (1) is chosen such that $\Phi = \Lambda = 45°$ at the chordwise position $r^1/l = 1$, where $R_l = U_l l/\nu = 10^6$ and $U_l = U_s \left(r^1 = l, r^3 = r^3_{\max} \right)$. We will employ two reference lengths for the presented figures, l and $\delta_l = \sqrt{\nu l/U_l}$.

First, we will restrict our study of optimal disturbances to a sub-critical chordwise interval, $0.005 \leq r^1/l \leq 0.25$, in order to study purely transient growth. Then, we will extend this interval to super-critical flows and study the evolvement of algebraically growing, non-modal disturbances into exponentially amplified modes.

From a physical point of view, it is desirable to start the calculations at the leading edge, in order to capture the process where vortical free-stream disturbances enters the boundary layer. There are however several problems associated with this upstream region. The Falkner–Skan–Cooke family of similarity solutions are discontinuous at the leading edge. For the normal velocity we have that $\lim_{r^1 \to 0} W \to \infty$, and in retarded flows it follows from equation (1) that $\lim_{r^1 \to 0} U^e \to \infty$. Despite these difficulties, which applies to the 2D case as well, Andersson et al. [1] and Luchini [18] independently carried out studies of transient growth in the Blasius boundary layer where the disturbances where introduced at the leading edge. Luchini [18] utilized a jump condition to solve the singularity problem, while Andersson et al. [1] carried out a study where the inception point was gradually moved towards the leading edge. They found that no dramatic changes occurs in the shape of the optimal disturbance or in the downstream response when the leading edge is approached, and concluded that the calculations could be initiated at the leading edge if the normal velocity is set to zero in the first calculation point. Neither Andersson et al. [1] or Luchini [18] did however address the problem that the boundary layer equations are not valid in this region. Levin & Henningson [16], who studied optimal disturbances in the Falkner–Skan boundary layers with favorable, zero and adverse pressure gradients, optimized the point of inception. They found that the maximum growth occurs when the disturbance is introduced into the boundary layer a significant distance downstream of the leading edge. The difficulties associated with the leading edge was therefore not considered.

For the swept flows studied herein, a new set of leading edge related problems arise in addition to those encountered in the 2D studies. The streamline angle, $\Phi = \arctan(V^e/U^e)$, is undefined at the leading edge in Falkner–Skan–Cooke boundary layers with non-zero pressure gradients. In accelerated flows we have $\lim_{r^1 \to 0} \Phi = 90°$, since $\lim_{r^1 \to 0} U^e = 0$. The axes ξ^1 and ξ^2 of the non-orthogonal coordinate system will thus collapse at the leading edge. In retarded flows, where $\lim_{r^1 \to 0} U_w \to \infty$, the limit of the streamline angle is $\lim_{r^1 \to 0} \Phi = 0°$. Both the accelerated and the retarded flow will undergo a very rapid transformation
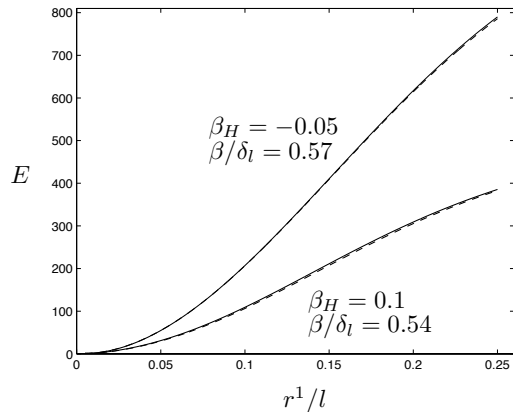
Figure 6: The energy growth of the optimal disturbance in the retarded and accelerated flow. $\Lambda = 45^o$
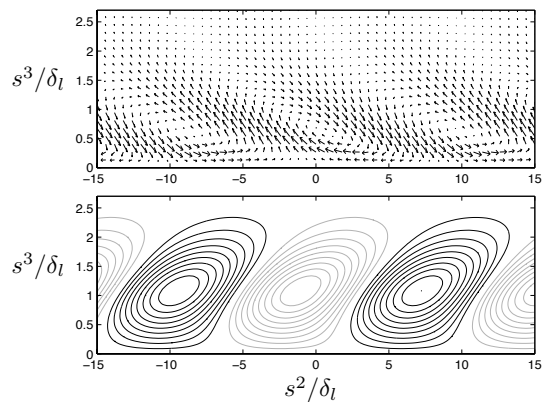
Figure 7: (a) Vector representation of optimal disturbances at $r^1/l = 0.005$, and (b) its downstream response at $r^1/l = 0.25$ projected onto the cross-flow plane (contours of positive, black, and negative, grey, streamwise velocity). $\Lambda = 45^0$, $\beta_H = 0.1$.

in the vicinity of the leading edge, where the streamline angle draws away from the extreme value at the leading edge. Furthermore, if it is assumed that the optimal disturbance takes the form of vortices more or less aligned with the external streamline, it is clear that the orientation of these vortices will vary rapidly when the point of inception is moved upstream towards the leading edge.

Due to the difficulties discussed above, the point of inception was set a small distance downstream of the leading edge, at $r^1/L = 0.005$. In figure 6, the energy growth of the optimal disturbances are shown as functions of the coordinate r^1 for both the accelerated and the retarded flow over the chordwise interval $0.005 \leq r^1/l \leq 0.25$. The initial disturbance is optimized to produce the maximum energy growth over this interval. As can be seen in figure 6, the retarded flow gives rise to twice the transient growth of the accelerated flow. Levin & Henningson [16], who studied optimal disturbances in the 2D Falkner–Skan boundary layers, also found that retarded flows gives rise to higher transient growth.
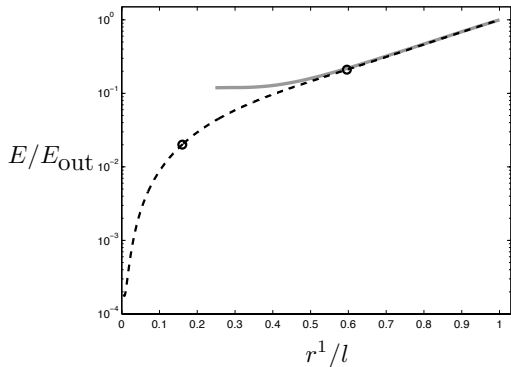
Figure 8: Energy growth of the optimal disturbance (black dashed line) and a cross-flow mode (grey line) with the same spanwise wavenumber, $\beta\delta_l = 0.34$.
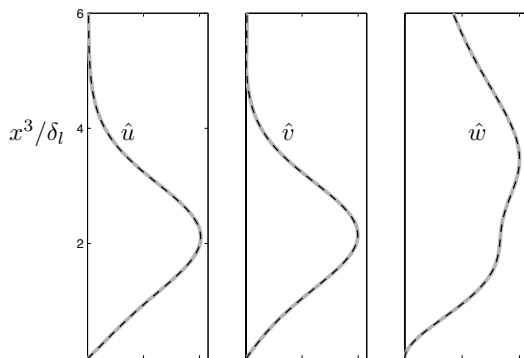
Figure 9: Downstream response to the optimal disturbance (dashed black line) at $r^1/l = 1.0$, compared to a PSE calculation of the cross-flow mode (grey line) with the same spanwise wavenumber, $\beta\delta_l = 0.34$.

Figure 7 shows a vector representation of the real part of the optimal disturbance in the cross-flow plane. It is apparent that the optimal disturbances take the form of counter-rotating vortices, similar to the optimal disturbances found in 2D flows. The vortices are however not symmetric as in 2D boundary layers, but tilted around the wall-normal axis. The vortices are tilted anti-clockwise in the accelerated flow and clockwise in the retarded flow (not shown here). This difference is likely related to the cross-flow component of the boundary layer, which changes sign with the pressure gradient. As the disturbances evolve downstream their orientation changes, the streaks at the end of the interval are therefore tilted clockwise in the accelerated flow and anti-clockwise in the retarded flow, i.e. the opposite of the initial disturbance. In 2D boundary layers the regions of transient and modal growth are well separated in the (ω, R)-plane, as noted by Luchini [18] in his study of transient growth in the Blasius boundary layer. The maximum transient growth occurs for stationary disturbances, and the growth decays rapidly with increasing frequency, while the exponential growth occurs for modal disturbances of relatively high frequen-

cies. In 3D boundary layers no such separation exists, since stationary modes can receive exponential amplification. Stationary cross-flow modes are a more common cause of transition than their traveling counterparts in free-flight conditions (Reed & Saric [19]). The stationary modes take the form of vortices, nearly aligned with the external streamline, and streaks of alternating high and low streamwise velocity. It is thus clear that this exponential instability resembles the algebraic instability described above. This is contrary to the situation in 2D boundary layer, where the modal disturbances are traveling waves and bears little resemblance to the disturbances associated with algebraic instability.

Now we consider the optimal disturbance in the accelerated flow, $\beta_{\mathrm{H}} = 0.1$, over the chordwise interval $0.005 \leq r^1/l \leq 1.0$, thus including super-critical flow. This allows us to study a scenario where transient growth pass over into exponential growth, to illuminate the differences and similarities between these instabilities. Corbett & Bottaro [6] considered sub- and super-critical Reynolds-numbers, comparing algebraically growing disturbances to exponentially amplified eigenmodes. They concluded that the algebraically growing disturbances are fed into cross-flow eigenmodes as the critical Reynolds-number is exceeded. The temporal analysis employed by Corbett & Bottaro [6] does however not allow a study where the downstream development of the disturbances can be monitored as they evolve from the sub- to the super-critical domain of the boundary layer. The spatial approach applied herein will however allow such a study, where both the algebraic growth and the subsequent exponential amplification of the disturbances is investigated.

Figure 8 shows the energy growth of the optimal disturbance with the spanwise wavenumber $\beta = 0.34/\delta_l$. For comparison, we have included data from a PSE calculation of a cross-flow mode with the same wavenumber, initiated at the point of neutral stability. It is clear that the algebraic growth of the optimal disturbance is followed by exponential growth, where the growth rate collapse with that of the modal disturbance. The reason is apparent from figure 9 which presents the amplitude functions of the cross-flow mode as well as the downstream response of the optimal disturbance at the end of the streamwise interval, $r^1/l = 1.0$. The close agreement proves that the optimal disturbance has evolved into a cross-flow mode. From figure 8 it can be concluded that the transition from algebraic to exponential amplification is a gradual process without any jumps in the growth rate. We thus conclude that the physical mechanism that drives the algebraic instability is similar to that responsible for the classical exponential instability, and that the algebraic disturbances are feed into exponentially amplified modes as the critical Reynolds-number is exceeded.

5 Conclusions

Two different approaches have been presented which both investigate optimal disturbances in spatially developing swept wing boundary layer flows.

The analysis presented in the first part of this paper is a "single-mode" approach to compute the algebraic growth of perturbations in three-dimensional spatially developing boundary layers based on a modified version of the modal analysis. It has been shown that when the interval, over which the optimal gain is computed, is large the solution can be wrtitten on a modal form times an Algebraic amplification Factor (AF). With a

properly defined normalization of the modal solution the AF is only a function of the corresponding left eigenvector. In the second part of the paper, a parabolic set of disturbance equations were employed to study algebraic and exponential instability in the Falkner–Skan–Cooke boundary layer. An adjoint-based optimization procedure was utilized to identify optimal disturbances, i.e. the initial disturbance which receives the greatest amplification over a given chordwise interval.

A comparison between these two approaches can be made considering the results presented in figures 5, 8 and 9. The so called "single mode approach" is based on an analysis which demonstrates that a perturbation in this kind of flow is dominated by a single mode. We have verified that the three velocity components plotted in figure 9, obtained from the PSE analysis, are indistinguishable from the components of the single mode. A direct comparison of the gain curve between the two approaches can not be made since the transient evolution of G is not captured in the single mode approach. However, the total amplification due to the transient growth can be compared by computing the algebraic amplification factor (AF), derived for the single-mode approach, for both cases. Based on the results given In figure 5 and 8, the energy gain from the single mode approach is slightly higher than the one computed using the PSE approach .

Acknowledgements

Bibliography

[1] P. Andersson, M. Berggren, and D.S. Henningson. Optimal disturbances and bypass transition in boundary layers. *Phys. Fluids*, 11:134–150, 1999.

[2] S. Bagheri and A. Hanifi. The stabilizing effect of streaks on tollmien-schlichting and oblique waves: A parametric study. *Phys. Fluids*, 19(7), 2007.

[3] K. Butler and V. Farrell. Three-dimensional optimal perturbations in viscous shear flow. *Phys. Fluids A*, 4(8):1637–1650, 1992.

[4] J. C. Cooke. The boundary layer of a class of infinite yawed cylinders. *Proc. Camb. Phil. Soc.*, 46:645–648, 1950.

[5] P. Corbett and A. Bottaro. Optimal perturbations for boundary layers subject to stream-wise pressure gradient. *Phys. Fluids*, 12:120–130, 2000.

[6] P. Corbett and A. Bottaro. Optimal linear growth in swept boundary layers. *J. Fluid Mech.*, 435:1–23, 2001.

[7] T. Ellingsen and E. Palm. Stability of linear flow. *Phys. Fluids*, 18(4):487–488, 1975.

[8] J. Floryan and W. Saric. Stability of Görtler vortices in boundary layers boundary layers. *AIAA J.*, 20(3):316–324, 1979.

[9] Byström M. G. *Optimal disturbances in boundary layer flows*. PhD thesis, KTH, 2007.

[10] P. Hall. The linear development of görtler vortices in growing boundary layers. *J. Fluid Mech.*, 130:41–58, 1983.

[11] A. Hanifi, D. S. Henningson, S. Hein, and M. Bertolotti, F. P.and Simen. Linear non-local instability analysis - the linear NOLOT code. *FFA TN*, 1994-54, 1994.

[12] A. Hanifi, P. J. Schmid, and D. S. Henningson. Transient growth in compressible boundary layer flow. *Phys. Fluids*, 8 (3):826–837, 1996.

[13] D. S. Henningson, A. Lundbladh, and A. Johansson. A mechanism for bypass transition from localized disturbances in wall-bounded shear flows. *J. Fluid Mech.*, 250:169–238, 1993.

[14] M. Högberg and D. S. Henningson. Secondary instability of cross-flow vortices in falkner-skan-cooke boundary layers. *J. Fluid Mech.*, 368:339–357, 1998.

[15] M. Landahl. A note on an algebraic instability of inviscid parallel shear flows. *J. Fluid Mech.*, 98(2):243–251, 1980.

[16] O. Levin and D. S. Henningson. Exponential vs algebraic growth and transition prediction in boundary layer flow. *Flow, Turbulence and Combustion*, 70:183–210, 2003.

[17] P. Luchini. Reynolds-number-independent instability of the boundary layer over a flat surface. *J. Fluid Mech.*, 327:101–115, 1996.

[18] P. Luchini. Reynolds-number-independent instability of the boundarylayer over a flat surface: optimal perturbations. *J. Fluid Mech.*, 404:289–309, 2000.

[19] H. L. Reed and W. S. Saric. Stability of three-dimensional boundary layers. *Ann. Rev. Fluid. Mech*, 21:235–284, 1989.

[20] A. Tumin. A model of spatial algebraic growth in a boundary layer subjected to a streamwise pressure gradient. *Phys. Fluids*, 13(5):1521–1523, 2001.

[21] A. Tumin and E. Reshotko. Spatial theory of optimal disturbances in boundary layers. *Phys. Fluids*, 13(7):2097–2104, 2001.